

Optimizing Chitosan production from insect-derived chitin

A. O. Lawal^{1,2}, E. E. Jasper^{3*}, J. C. Onwuka^{4*}, K. O. Ijege², F. C. Emeachi² and A. T. Adeniyi²

¹Department of Chemistry, Kaduna State University, Kaduna State, Nigeria

²Department of Applied Chemistry, Kaduna Polytechnic, Kaduna State, Nigeria

³Department of Chemistry, Dennis Osadebay University, Asaba, Delta State, Nigeria

⁴Department of Science Laboratory Technology, Federal University of Lafia, Nasarawa State, Nigeria

ARTICLE INFO

Received: 18 June 2025

Revised: 20 July 2025

Accepted: 06 August 2025

eISSN 2224-7157/© 2025 The Author(s).
Published by Bangladesh Council of
Scientific and Industrial Research
(BCSIR).

This is an open access article under the
terms of the Creative Commons Non
Commercial License (CC BY-NC)
(<https://creativecommons.org/licenses/by-nc/4.0/>)

Abstract

Chitosan is an emerging raw material with increasing global demand, traditionally derived from crustaceans. Its production faces challenges such as high cost and inconsistent yields, necessitating the search for new chitosan precursors. This study investigates *Melanoplus differentialis*, a differential grasshopper, for sustainable chitosan production. Chitin was extracted from *M. differentialis* via sequential demineralization, deproteination, and decolorization, and then deacetylated. Response Surface Methodology (RSM), using the Box-Behnken design, was used to optimize NaOH concentration, NaOH:Chitin ratio, and deacetylation time. Statistical analysis identified NaOH concentration as the most significant factor influencing yield. The optimal process conditions of 40.5% NaOH, 16.8 mL/g NaOH: chitin ratio, and 69.3 minutes resulted in 60.62±0.79% chitosan yield. FTIR confirmed the transformation of chitin to chitosan. This study shows *M. differentialis* as a promising, unconventional chitosan precursor.

Keywords: Chitin; Chitosan; Deacetylation; Optimization; *Melanoplus differentialis*; RSM

DOI: <https://doi.org/10.3329/bjsir.v60i3.82280>

Introduction

Chitosan is a biopolymer obtained from the partial deacetylation of the natural polysaccharide chitin, which is primarily isolated from crustaceans, mollusks, and fungi (Pakizeh *et al.* 2021; Aranza *et al.* 2021). Chitosan is the second most abundant biopolymer after cellulose (Choi *et al.* 2016); it is mainly composed of β -(1→4)-linked units of either D-glucosamine or N-acetyl-D-glucosamine (Fig. 1). Chitin presents a variety of advantageous properties, including biocompatibility, biodegradability, low toxicity, and antimicrobial activity (Elieh-Ali-Komi and Hamblin, 2016; Reshad *et al.* 2021) making it very important in a range of industrial applications. This multifunctional property of the molecule can be attributed to the presence of a large number of reactive amino and hydroxyl groups in its structure. All these traits make chitosan a biopolymer of economic interest. The increasing global demand for chitosan and its by-products as

a result of their versatile applications in new research fields necessitates the discovery of new chitosan precursors. This study investigates the potential of *Melanoplus differentialis*, a differential grasshopper, as a chitosan precursor.

Chitosan stands out in nano medicine for its biocompatibility, making it a great fit for various medical applications like drug delivery systems, tissue engineering, and wound healing (Frigaard *et al.* 2022; Triunfo *et al.* 2022; de Sousa *et al.* 2020; Jiménez-Gómez and Antonio, 2020). It is also biodegradable, thus reducing issues of long-term environmental pollution. Chitosan is gaining traction in sustainable practices, such as wastewater treatment, where it effectively adsorbs heavy metals and other pollutants (Verma and Quraishi, 2021; Hahn *et al.* 2020).

*Corresponding author's e-mail: enebi.jasper@dou.edu.ng

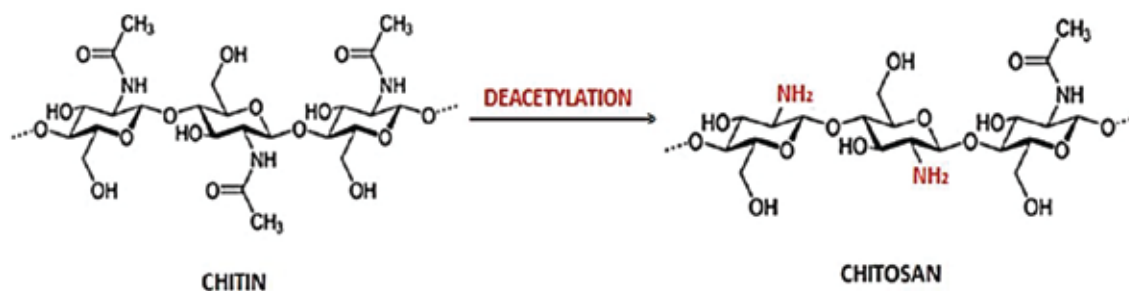


Fig. 1. Molecular structures of chitin and chitosan (Struszczyk, 2002)

The applications have been found in crop protection (Wang *et al.* 2024; Teixeira-Costa and Andrade, 2021) and textile technology (Elamri *et al.* 2023).

Traditionally, crustaceans are used for commercial chitin production; however, lately, insects are being recognized as a more sustainable option. Unlike crustaceans, whose use could lead to environmental concerns such as overfishing, high processing costs, and inconsistent yields (Machado *et al.* 2024; Zainol Abidin *et al.* 2020), insects provide a more reliable and eco-friendly option. Insects reproduce quickly, have short life spans, and are not affected by seasonal changes because they can be bred all through the year (Triunfo *et al.* 2022). They also require fewer resources like land, water, and feed, and produce lower greenhouse gas emissions (Espinosa-Solís *et al.* 2024). Chitin derived from insects has advantages in consideration of cost and zero waste generation (Mei *et al.* 2024; Rehman *et al.* 2023).

The synthesis of chitosan via the deacetylation of chitin is influenced by several factors such as time, temperature, alkali volume, and alkali-to-chitin ratio. The utilization of the Response surface methodology (RSM), a multivariate statistical technique, serves to optimize analytical processes in which a response of interest is influenced by several factors. It enables simultaneous optimization of the levels of these factors to achieve the best process performance. RSM enables the simultaneous optimization of multiple factors by using polynomial regression models fitted to experimental data, enabling precise statistical predictions and process optimization (Bezerra *et al.* 2008). Unlike the traditional one-factor-at-a-time (OFAT) approach, RSM allows for the efficient study of factor interactions through multifactor experiments, reducing cost and time while enhancing the understanding of factor interactions for optimal performance. According to Montgomery (2017), the technique typically consists of three main steps: conducting statistically designed experiments, developing a regression model that approximates the true response

surface, and assessing the model to determine optimal conditions. When modeling quadratic responses, the most widely used experimental designs in RSM are Central Composite Design (CCD) and Box-Behnken Design (BBD), which offer efficiency and accuracy (Ferreira *et al.* 2007; Myers *et al.* 2016). RSM has been especially helpful in bioprocess optimization, where improving yield and quality requires the simultaneous control of multiple inter-dependent variables.

Box Behnken design (BBD), a type of RSM, was employed in this study. In addition to optimizing the factor settings, it evaluates the interaction effect of NaOH concentration, time, and the ratio of NaOH to chitin in relation to the yield of chitosan. The BBD was chosen over other Response surface methodologies like the Central Composite Design because it avoids factor combinations at extreme settings, enhancing laboratory safety, especially when handling reagents like highly alkaline NaOH. It also improves environmental efficiency while providing statistically valid results. The efficacy of BBD has also been proven with crustacean shells and stems of mushrooms as chitin sources (Huang and Tsai, 2020; Amoo *et al.* 2019; Gamal *et al.* 2016; Vaingankar and Juvekar, 2014). The optimization method reiterates the potential of derived biopolymers of insects (Kaya *et al.* 2015). The optimization of the development of pea-starch-chitosan novel edible product was also enabled by the application of Box-Behnken RSM (Thakur *et al.* 2017).

Synthesized polymers are largely implicated in fouling the environment owing to environmental disposal challenges due to their non-biodegradability and enormous space occupation (Bello and Olafadehan, 2021). Biopolymers such as chitosan are a suitable replacement for such synthesized variants because of their properties of biocompatibility, non-toxicity, and biodegradability. The search for such biopolymers addresses an important research gap. Recent research reports that fungal-derived chitosan is superior to that derived from

crustacean sources also stimulated the direction this research. (Milbreta *et al.* 2025; Almeida *et al.* 2023).

This research focuses on optimizing the yield of chitosan obtained from *Melanoplus differentialis* and studying the influence of factors such as NaOH concentration, NaOH: Chitin ratio, and deacetylation time. using the Box; Behnken design. The chitin is extracted from the insect by a series of demineralization, deproteination, and decolorization processes, after which it is deacetylated. The successful transformation of the precursor to chitosan was confirmed using Fourier Transform Infrared spectrophotometry (FTIR).

room temperature with a 3.5 % sodium hypochlorite solution at a solvent-to-solid ratio of 10:1(w/v). The decolorized residue was then rinsed thoroughly with deionized water until neutral. The resultant product was chitin.

Synthesis of Chitosan via Deacetylation of Chitin Derived from Melanoplus differentialis Using the Box-Behnken Design (BBD)

To assess the effects and interactions of process parameters on chitosan yield, a three-factor three-level

Table I. Factor levels in the Box-Behnken experimental design for the production of chitosan from *M. differentialis*

Factor	Code	Box- Behnken levels		
		Low(-1)	Middle (0)	High (+1)
NaOH concentration (%)	A	30	40	50
Solvent: solid ratio (mL/g)	B	10	15	20
Deacetylation time(min)	C	30	60	90

Materials and methods

Melanoplus differentialis was used as the chitin precursor in this research. Reagents used include NaOH, HCl, and sodium hypochlorite, which were all Analar grade. All solutions for this study were prepared using de-ionized water.

Extraction of chitin from melanoplus differentialis

Dried *Melanoplus differentialis* samples from the Tudun Wada area of Kaduna Metropolis in Nigeria were initially washed with tap water to remove dust. The cleaned samples were then oven-dried at 100°C until a constant weight was achieved. Dried *M. differentialis* was converted to chitin via demineralization and deproteinization using acid and alkaline treatment, respectively. For demineralization, 10 g of *M. differentialis* was placed in 4% HCl at room temperature for 24 hrs, with a solvent-to-solid ratio of 15:1 (v/w). The demineralized residue was then treated with 2% NaOH for deproteinization at a temperature of 70°C for 2 hrs while stirring continuously, at a solvent-to-solid ratio of 15: 1 (v/w). The residue obtained after filtering was washed with de-ionized water until the pH reached 7 and then dried in an oven. The dried residue was thereafter decolorized at

Box-Behnken experimental design was used, namely (i) NaOH percent concentration (30-90 %), (ii) solvent: solid ratio (10-20 mL/g), and (iii) deacetylation time (30 -90 min) (designated as A, B, and C, respectively for statistical computations). Details of these independent variables and their experimental levels are presented in Table I.

The levels of the factors were based on previous studies and preliminary results from the experiments carried out. To optimize chitosan yield, 15 experiments were generated from the BBD with 3 replicates of the center points. The chitosan synthesis involved the reaction of 1g of chitin with 30, 40, and 50% NaOH, varying solvent/solid ratios of 10:1 v/w, 15:1 v/w and 20:1 v/w and varying reaction times of 30, 60 and 90 minutes at a fixed temp of at 80°C, as shown in Table II.

Residual NaOH was removed by washing the chitosan samples thoroughly with deionized water until the filtrate's pH reached 7. The prepared chitosan was bleached using 3.5 % sodium hypochlorite solution, to remove its brownish colour. The samples were dried at 100°C for 1 hour and then pulverized. The processed chitosan was stored in sealed plastic bottles.

Table II. Box–Behnken experimental design matrix Chitosan synthesis optimization

Run	Chitosan preparation variables			
	A: NaOH concentration (%)	B: Solvent: Solid Ratio (mL/g)	C: Deacetylation Time (min)	
1	30	15	30	
2	50	20	60	
3	50	10	60	
4	50	15	30	
5	50	15	90	
6	40	10	90	
7	40	20	90	
8	40	20	30	
9	30	15	90	
10	30	10	60	
11	40	15	60	
12	40	15	60	
13	40	10	30	
14	40	15	60	
15	30	20	60	

Assessment of the performance of the chitosan synthesis method

The performance of the chitosan synthesis method was evaluated based on the percentage yield of the chitosan samples. The yield was calculated as the percentage of the weight of the dried chitosan relative to the initial weight of chitin, according to the formula shown in Equation 1.

$$\text{chitosan yield (\%)} = \left(\frac{\text{mass of chitosan}}{\text{mass of chitin}} \right) \times 100 \quad (1)$$

Optimization and statistical analysis of the chitosan synthesis

BBD optimization was enabled by Design Expert 13 and statistical analysis of variance. The validity of the optimal conditions was confirmed by synthesizing chitosan under the optimized conditions and comparing the experimental yield with the values predicted by the software.

*FTIR spectroscopic analysis of the *M. differentialis* chitosan and its precursors*

The surface functional groups of precursor, chitin, and chitosan were qualitatively analyzed using Fourier Transform Infrared (FTIR) spectroscopy (FTIR-CARY 630, Agilent Technologies) within the range of 4000–650 cm^{-1} .

Results and discussion

*Chitosan yield from *M. differentialis* (MD-chitosan) using the BBD*

Table III presents the experimental yields of chitosan obtained from *M. differentialis* chitin, ranging from 47.2 to 77.6% and the associated model-predicted yields ranging from 48.1 to 75.5%. These results were obtained using various combinations of the factors that influence the synthesis process.

Regression analysis and analysis of variance (ANOVA)

The second-order polynomial regression equation derived from the software, depicting the relationship between the response, chitosan yield, and the three independent factors, is presented in Equation 2, in terms of the coded factors with the insignificant terms already removed.

$$\text{Chitosan Yield} = +63.63 - 9.96A - 2.63B - 2.74C - 2.82AB - 1.45AC - 4.58BC \quad (2)$$

The equation in coded form can be used to make predictions about the response for given levels of each factor. By default, the high levels of the factors are coded as +1, and the low levels are coded as -1. The coded equation is useful for

Table III. *Melanoplus differentialis* chitosan yield

Run	Chitosan preparation factors			Response		
	A:NaOH %	B:Solvent:solid ratio(mL/g)	C: Deacetylation time (min)	Actual Yield %	Predicted Yield %	
1	30	15	30	77.6	75.5	
2	50	20	60	47.2	48.1	
3	50	10	60	60.1	59.0	
4	50	15	30	60.4	62.8	
5	50	15	90	48.0	50.1	
6	40	10	90	69.2	68.2	
7	40	20	90	56.8	53.8	
8	40	20	30	67.4	68.4	
9	30	15	90	71.0	72.9	
10	30	10	60	74.2	73.3	
11	40	15	60	60.4	57.9	
12	40	15	60	59.8	63.4	
13	40	10	30	61.5	64.5	
14	40	15	60	64.0	62.8	
15	30	20	60	72.6	73.7	

Table IV. ANOVA for yield of chitosan from *M. differentialis* chitin

Source	Sum of squares	Df	Mean Square	F-value	p-value	
Model	1033.14	6	172.19	26.10	< 0.0001	significant
A-NaOH concentration	794.01	1	794.01	120.33	< 0.0001	
B-Solvent: solid ratio	55.13	1	55.13	8.35	0.0202	
C-Deacetylation time	59.95	1	59.95	9.09	0.0167	
AB	31.92	1	31.92	4.84	0.0590	
AC	8.41	1	8.41	1.27	0.2916	
BC	83.72	1	83.72	12.69	0.0074	
Residual	52.79	8	6.60			
Lack of Fit	44.15	6	7.36	1.70	0.4150	not significant
Pure Error	8.64	2	4.32			
Cor Total	1085.93	14				
Std.Dev.	2.57		R ²	0.9514	Adeq Precision	15.1943
Mean	63.63		Adjusted R ²	0.9149		
C.V. %	4.04		Predicted R ²	0.7823		

identifying the relative impact of the factors by comparing the factor coefficients. The coefficients in the model equation indicate the magnitude and extent of influence each factor has on the response. A positive sign shows a positive correlation, while an inverse relationship is signified by a negative coefficient. Optimization was performed using Equation 1. This model shows that increases in NaOH concentration (A), solvent-to-solid ratio (B), deacetylation time (C), and the interaction of the factors do not significantly increase the chitosan yield, implying that increases in these terms lead to a decrease in chitosan yield. This is an indication that the optimum conditions for the synthesis of chitosan from the insect-derived chitin would not be on the very high side of the coded factors.

Analysis of Variance (ANOVA) was used to assess the statistical significance of the regression models, illustrating the effects of each process factor and their interactions on the response. It evaluates the accuracy with which the model equation represents the actual relationship between the response and significant factors. The ANOVA results for the response surface quadratic model of chitosan yield after excluding insignificant quadratic and interaction terms are shown in Table IV. ANOVA employs Fisher's F-test (F) and $\text{Prob} > F$ (p) values to assess the significance of process factors. A factor with higher F-values and lower p-values is considered more significant. Specifically, p-values less than 0.05 indicate that the corresponding factor has a statistically significant impact on the chitosan yield. Generally, a high F-value combined with a p-value below 0.05 confirms the significance of a regression model or an independent variable.

The model shows that the individual contributions of the factors A, B, and C, as manifested by the negative coefficients, are significant with p-values, 0.0001 (NaOH concentration), 0.0202 (solvent: solid ratio), and 0.0167 deacetylation time (Table IV). The interaction term BC (p-value, 0.0074) was also significant. The quadratic terms were not significant in the model and were therefore removed from the model equation. However, the contributions of the two-factor interactions (2FI) of AB and AC were retained even though their contributions were not significant, as depicted by p-values of 0.0590 and 0.2916 for AB and AC, respectively. This retains and improves the model's robustness and accounts for potential factor interactions. The model constant, + 63.63, is the chitosan yield at the baseline conditions, corresponding to the coded factors at the zero level. The most significant factor at $p < 0.05$ is NaOH concentration (A), which tends to reduce the chitosan yield by 9.96% when the NaOH concen-

tration is varied by one unit. The overall F-value of 26.10 implies that the model is significant, indicating that there is only a 0.01% chance that an F-value this large could occur due to noise. P-values less than 0.0500 mean that the model terms are significant.

The Lack of Fit F-value of 1.70 symbolically implies that the Lack of Fit is not significant relative to the pure error. There is therefore a 41.50% chance that a Lack of Fit F-value of this magnitude could occur due to noise. It is noteworthy that a non-significant lack of fit is good for the model. The predicted R^2 of 0.7823 is in reasonable agreement with the adjusted R^2 of 0.9149 because the difference is less than 0.2. Adequate Precision measures the signal-to-noise ratio. A ratio greater than 4 is desirable. The ratio of 15.1943 indicates an adequate signal, meaning that this model can be used to navigate the design space. A coefficient of variance (CV) of 4.04%, which is much less than 10%, shows that the model is reasonably reproducible and that the experimental values show good accuracy. The model adequacy was determined by the Adeq precision. The Adequate precision value of 15.1943 (Table IV) indicates that the model has good precision and fitness with the experimental values, thereby ensuring reproducibility of the results.

Among the factors, the linear term A (NaOH concentration) was found to have the most significant influence on chitosan yield, with an F-value of 120.33. The linear terms B (solvent-to-solid ratio) and C (deacetylation time), and the 2-way interaction term BC, were also significant. The order of significance is as follows: $A > BC > C > B$, indicating that the solvent-to-solid ratio has the least influence on chitosan yield. However, the interaction effect of the solvent-to-solid ratio and deacetylation time (BC) suggests the gradual penetration of the NaOH into the chitin particles for increased surface area of contact as time progresses for optimal reaction. Overall, the statistical findings support predictive capability of the model within the range of the variables studied.

The extent of agreement of the experimental and predicted values of the chitosan yield is illustrated in Figure 2. The scatter plot displays the experimental and predicted values in close association with the regression line, thereby validating capability of the model for effective and efficient prediction of the chitosan yield. The degree of closeness of the points to the regression line indicates the level of closeness of the experimental values to the model-predicted values of the chitosan yield. This further validates and confirms the accuracy of the developed model.

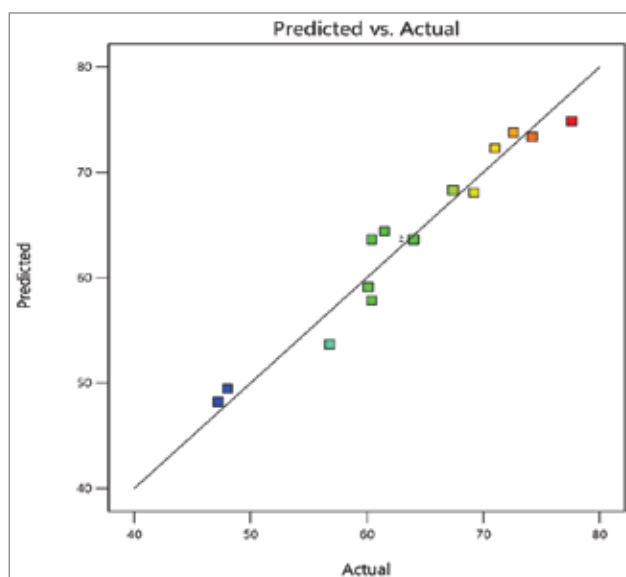


Fig. 2. Plot of predicted and actual values of the chitosan yield

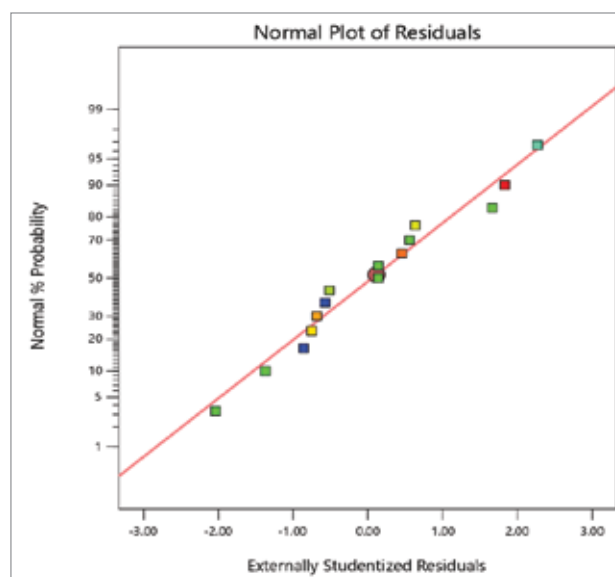


Fig. 3. Diagnostic normal probability plot of residual analysis

Table V. Comparison of experimental and predicted chitosan yields

Run Order	Actual Value	Value	Residual	Leverage	Externally Studentized Residuals
1	64.00	63.63	0.3733	0.067	0.141
2	77.60	74.88	2.72	0.567	1.833
3	72.60	73.79	-1.19	0.567	-0.679
4	60.40	63.63	-3.23	0.067	-1.370
5	60.40	57.85	2.55	0.567	1.666
6	74.20	73.39	0.8108	0.567	0.455
7	47.20	48.21	-1.01	0.567	-0.574
8	61.50	64.41	-2.91	0.567	-2.033
9	69.20	68.09	1.11	0.567	0.632
10	67.40	68.31	-0.9142	0.567	-0.515
11	71.00	72.30	-1.30	0.567	-0.748
12	60.10	59.11	0.9858	0.567	0.557
13	56.80	53.69	3.11	0.567	2.266
14	64.00	63.63	0.3733	0.067	0.141
15	48.00	49.48	-1.48	0.567	-0.859

Table V further supports the observation from Figure 2, which suggests a strong agreement between predicted and experimental values as evidenced by the small residuals and absence of outliers.

Figure 3 presents the diagnostic normal plot of residual analysis for validating the model developed for predicting the

chitosan yield. The predicted and experimental data points were very close and showed a straight-line relationship that confirmed the good agreement between the experimental and predicted yields of chitosan.

The relationship between residuals and probability verifies the assumption that model errors are normally distributed and

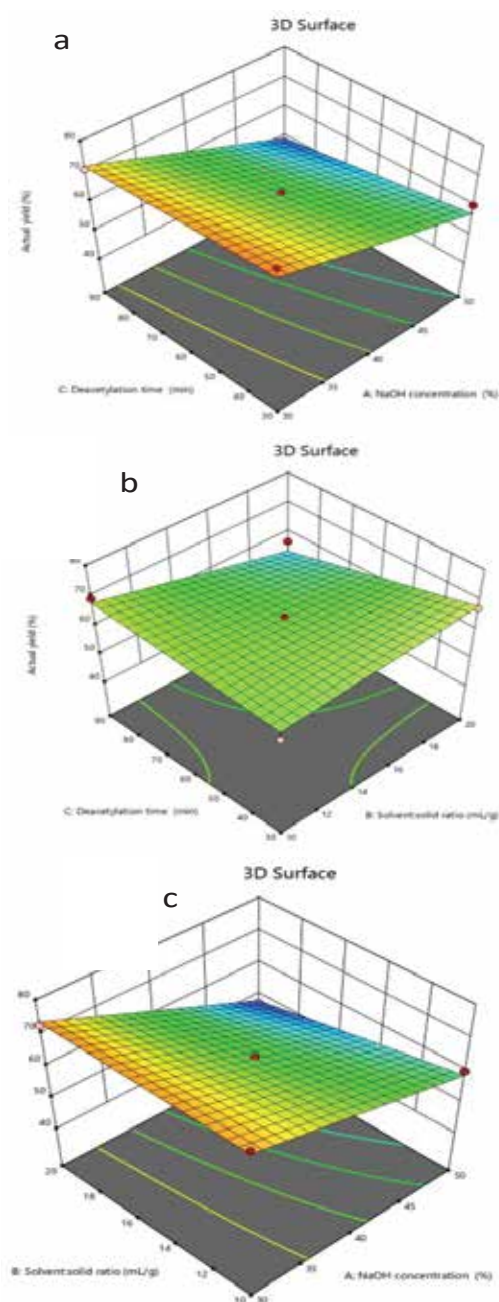


Fig. 4. Response surface plots of chitosan yield at holding values of solvent:solid ratio 15, deacetylation time, 60 min and 40 % NaOH concentration

indicating that the model predictions are well-fitted. The Adjusted R^2 of 0.9149 means that the model accounts for 91.49% of the variation in chitosan yield with the factors and interaction of factors. The display of the assessment of the normal distribution of the residuals in Figure 3 illustrates that the data points in the plot are linear, confirming the residuals as normally distributed. All data

thus represent a good fit, having the experimental values falling within the limit. This highlights that the unexpected errors that may be in the model are minimal.

Response surface plots

Design Expert 13 generated the three-dimensional response surface plots for the chitosan yield, as illustrated in Figure 4a-c. These plots depict the interactions between two variables while holding the third variable constant. The 3-D response surface plots show a graphical representation of the effects of each independent factor on the yield of chitosan across the whole design space (Fig. 4a-c).

Figure 4a depicts the interaction effect of NaOH concentration (A) and deacetylation time (C) on the yield of chitosan. At a fixed solvent to solid ratio of 15, 74.44% optimum yield of chitosan was obtained from 30.17% NaOH concentration at 30.40 min, deacetylation time. The interaction effect of the solvent: solid ratio and deacetylation time, on chitosan yield is shown in Figure 4b. The 3D surface plot revealed that 40% NaOH concentration, solvent: solid ratio of 19.8mL/g and deacetylation time of 30.8 min produced 67.76% of chitosan. This is because over time, a higher solvent-to-solid ratio intensifies the interaction between alkali and chitin, leading to complete deacetylation of the chitin structure and decreasing the chitosan yield. These results are similar to those reported by Dinculescu *et al.* (2023), who found that higher NaOH concentrations reduced chitosan yield from *Rapana venosa* egg capsule waste. However, at an increased deacetylation time of 60min, and reduced concentration of NaOH (30.02%), the chitosan yield increased to 73.48% at solvent:solid ratio of 19.86. This potentially highlights the fact that the desired NaOH concentration for optimum yield of chitosan from the insect-derived chitin falls around the lower limit of the coded value and center point.

Optimization and validation

In this study, the experimental value of the yield of chitosan agreed substantially with that predicted by the software, thus validating the determined optimal conditions for its synthesis. Adeyi *et al.* (2018) and Ngomo *et al.* (2024) have optimized chitosan yield from shrimp shells using variants of RSM. Amoo *et al.* (2019) optimized the extraction of biopolymers, chitin and chitosan, from *Penaeus notialis* shells, using the BBD,

obtaining 26.08% and 16.93% yield of chitin and chitosan, respectively, under optimal conditions. Similarly, Ibrahim *et al.* (2022) optimized the synthesis of low molecular weight nano-chitosan from waste white shrimp shells via the CCD and RSM, while Noura El-Far *et al.* (2021) and Olafed-ehan *et al.* (2020) have also confirmed the effectiveness of RSM for optimizing synthesis.

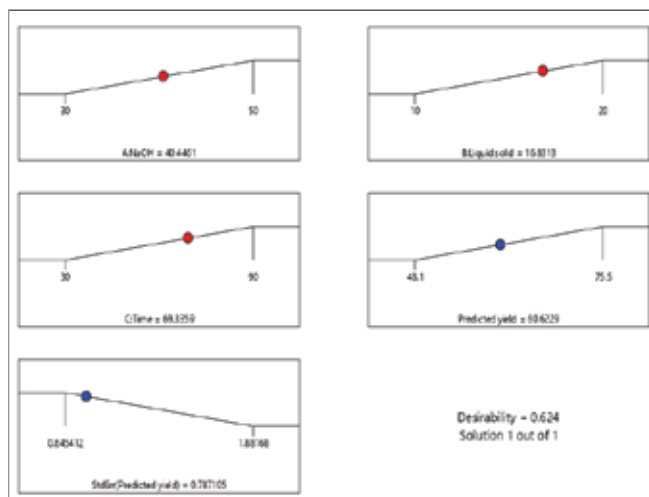


Fig. 5. Model desirability plot for the optimization of chitosan synthesis from chitin derived from *M. differentialis*

Fig. 5. shows the desirability plot for numerically optimized process conditions for the preparation of chitosan from chitin derived from *M. differentialis*. The predicted optimum factors for optimum yield of chitosan are NaOH concentration of 40.45%, solvent: solid ratio of 16.83 mL/g, and deacetylation time of 69.34 min. The predicted yield of chitosan from the optimized factors is 60.62%, with a desirability factor of 0.624.

FTIR spectroscopic analysis of the *M. differentialis* Chitosan and its precursors

Fourier Transform Infrared (FTIR) spectroscopy is a technique that is capable of providing a detailed characterization of the structural changes that occur during the conversion of biomass precursors to a desired end product. Figure 6 reveals major changes in the spectrum of the precursor, chitin and chitosan when compared to one another.

The *M. differentialis* FTIR spectrum (Fig 6 a) contains some distinct peaks at 3272.6 cm⁻¹, corresponding to characteristic absorption peak of O-H and N-H symmetric stretching vibration, suggesting the presence of hydroxyl

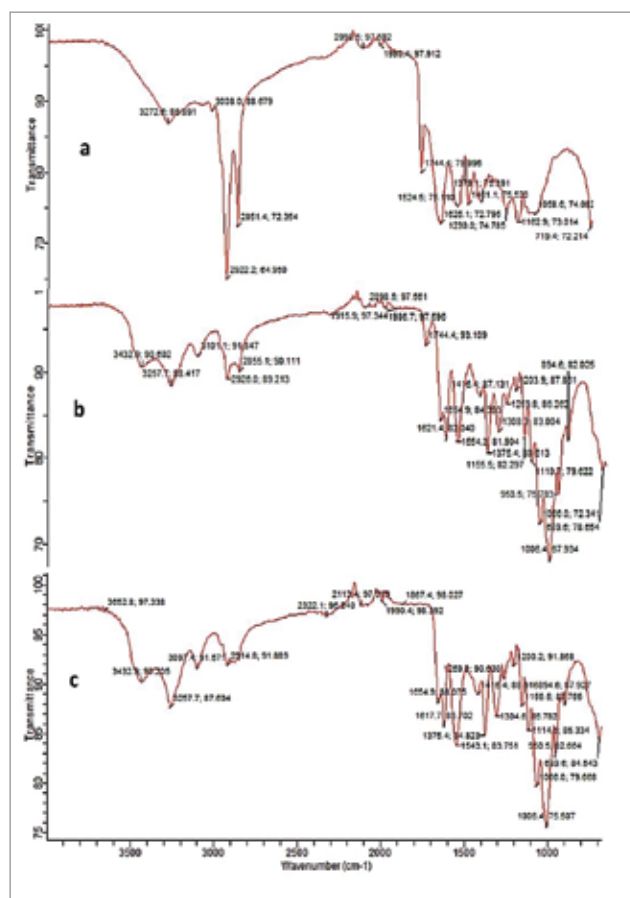


Fig. 6. FTIR Spectra of a) *Melanoplus differentialis* b) *Melanoplus differentialis* chitin and c) *Melanoplus differentialis* chitosan

and amine functional groups, 2922.2 cm⁻¹ (carboxylic acid O-H), and 2851.4 cm⁻¹ (symmetric C-H stretching vibration from CH₂ and CH₃), which indicates the presence of methyl and methylene groups. When this spectrum is compared to chitin (Fig. 6b), a noticeable drop in peak intensity was observed, resulting from the demineralization and deproteinization processes that chitin goes through. The peak at 1654.9 cm⁻¹ however, remains, representing the C=O stretching vibration of amide I. This peak is a strong indicator of the N-acetyl group in chitin that stays intact even after removing other components. Fig 6 c bears a close resemblance with chitosan as evidenced by the broad bands at 3200-3550cm⁻¹, the amide I peak at 1650 cm⁻¹, and the amide II band at 1580 cm⁻¹, which corresponds to hydroxyl, amine and partially acetylated glucosamine units of chitosan respectively (Elhaes *et al.*, 2024; Tiama *et al.* 2023)

The peaks at 1000-1200cm⁻¹ are indicative of the C-O-C and C-N stretch, further confirming that the spectrum presents chitosan. The distinct spectral characteristics of the *M. differentialis* spectrum showcase its original chemical makeup, with the alterations in the other spectra confirming the successful transformation of the precursor to a new product.

Conclusion

This study reveals that *M. differentialis* can be used as a viable precursor for chitosan production. The chitosan synthesis process was successfully optimized using Response surface methodology, and the influence of three independent factors, NaOH concentration, solid: solvent ratio, and reaction time, on the chitosan yield was explained. A 60.62% chitosan yield was obtained at optimal conditions of NaOH concentration of 40.45%, solvent: solid ratio of 16.83mL/g, and deacetylation time of 69.34min, being the most statistically significant factors influencing the chitosan yield. FTIR spectral characterization confirmed the transformation of the insect-chitin precursor to chitosan. Overall, RSM has proved to be effective for the optimization of chitosan synthesis parameters, resulting in high product yield. This research will promote insect farming and bio-derived value, thereby supporting sustainable industries development and environmentally responsible innovations.

Acknowledgement

The authors are grateful to the Multi-user lab of the Ahmadu Bello University and the Department of Applied Chemistry, Kaduna Polytechnic, where this research was carried out.

References

- Adeyi A, Oloje AO and Giwa A (2018), Statistical optimization of chitosan extraction from shrimp shells using response surface methodology, *ABUAD J Eng Res Dev* **1**(1): 8-17.
- Almeida RR, Pinto NAR, Soares IC, Clarindo Ferreira LB, Lima LL, Leitão AA and Guimarães LGL (2023), Production and physicochemical properties of fungal chitosans with efficacy to inhibit mycelial growth activity of pathogenic fungi, *Carbohydr Res*. **525**: 108762. <https://doi.org/10.1016/j.carres.2023.108762>
- Amoo KO, Olafadehan OA and Ajayi TO (2019), Optimization studies of chitin and chitosan production from *Penaeus notialis* shell waste, *Afr J Biotechnol* **18**(27): 670-688. <https://doi.org/10.5897/AJB2019.16861>
- Aranza I, Alcántara AR, Civera MC, Arias C, Elorza B, Caballero HC and Acosta N (2021), Chitosan: An overview of its properties and applications, *Polymers* (Basel) **13**(19): 3256. <https://doi.org/10.3390/polym13193256>
- Bezerra MA, Santelli RE, Oliveira EP, Villar LS and Escalreira LA (2008), Response surface methodology (RSM) as a tool for optimization in analytical chemistry, *Talanta* **76**: 965. <https://doi.org/10.1016/j.talanta.2008.05.019>
- Bello VE and Olafadehan OA (2021), Comparative investigation of RSM and ANN for multi-response modeling and optimization studies of derived chitosan from *Archachatina marginata* shell, *Alexandria Eng J* **60**: 3869-3899. <https://doi.org/10.1016/j.aej.2021.02.047>
- Choi C, Nam JP and Nah J (2016), Application of chitosan and chitosan derivatives as biomaterials, *J Ind Eng Chem* **33**: 1. <https://doi.org/10.1016/j.jiec.2015.10.028>
- de Sousa Victor R, da Cunha Santos AM, de Sousa BV, de Araújo Neves G, de Lima Santana N and Menezes R (2020), A review on chitosan's uses as biomaterial: Tissue engineering, drug delivery systems, and cancer treatment, *Materials* **13**: 4995. <https://doi.org/10.3390/ma13214995>
- Dinculescu D, Gîjiu CL, Apetroaei MR, Isopescu R, Rău I and Schröder V (2023), Optimization of chitosan extraction process from *Rapana venosa* egg capsules waste using experimental design, *Materials* **16**(2): 525. <https://doi.org/10.3390/ma16020525>
- Elamri A, Zdiri K, Hamdaoui M and Harzallah O (2023), Chitosan: A biopolymer for textile processes and products, *Text Res J* **93**(5-6): 1456-1484. <https://doi.org/10.1177/00405175221127315>
- Elhaes H, Ezzat HA, Ibrahim A, Samir M, Refaat A and Ibrahim MA (2024), Spectroscopic, Hartree-Fock and DFT study of the molecular structure and electronic properties of functionalized chitosan and chitosan-graphene oxide for electronic applications, *Opt Quant Electron* **56**: 458. <https://doi.org/10.1007/s11082-023-05978-0>
- Elich-Ali-Komi D and Hamblin MR (2016), Chitin and chitosan: Production and application of versatile biomedical nanomaterials, *Int J Adv Res*. **4**(3): 411-427.

- Espinosa-Solís A, Velázquez-Segura A, Lara-Rodríguez C, Martínez LM, Chuck-Hernández C and Rodríguez-Sifuentes L (2024), Optimizing chitin extraction and chitosan production from house cricket flour, *Processes* **12**(3): 464. <https://doi.org/10.3390/pr12030464>
- Ferreira SLC, Bruns RE, Ferreira HS, Matos GD, David JM, Brandão GC and Souza AS (2007), Box-Behnken design: An alternative for the optimization of analytical methods, *Analytica Chimica Acta* **597**(2): 179-186. <https://doi.org/10.1016/j.aca.2007.07.011>
- Frigaard J, Jenses JL, Galtung HK and Hiorth M (2022), The potential of chitosan in nanomedicine: An overview of the cytotoxicity of chitosan-based particles, *Front Pharmacol* **13**: 880377. <https://doi.org/10.3389/fphar.2022.880377>
- Gamal RF, El-Tayeb TS, Raffat EI, Ibrahim HM and Bashandy AS (2016), Optimization of chitin yield from shrimp shell waste by *Bacillus subtilis* and impact of gamma irradiation on production of low molecular weight chitosan, *Int J Biol Macromol* **291**: 598-608. <https://doi.org/10.1016/j.ijbiomac.2016.06.008>
- Hahn T, Tafi F, Paul A, Salvia R, Falabella P and Zibek Z (2020), Current state of chitin purification and chitosan production from insects, *J Chem Technol Biotechnol*, **95**: 2775-2795. <https://doi.org/10.1002/jctb.6533>
- Huang Y and Tsai H (2020), Extraction of chitosan from squid pen waste by high hydrostatic pressure: Effects on physicochemical properties and antioxidant activities of chitosan, *Int J Biol Macromol* **160**: 677-687. <https://doi.org/10.1016/j.ijbiomac.2020.05.252>
- Ibrahim AA, Jimoh A, Diekola YM and Auta M (2022), Extraction of nano-chitosan from waste white shrimp shells for removal of phenol from refinery wastewater: Optimization of chitosan synthesis and phenol adsorption, *ABUAD J Eng Res Dev* **5**(1): 93-109.
- Jiménez-Gómez CP and Antonio J (2020), Chitosan: A natural biopolymer with a wide and varied range of applications, *Molecules* **25**(17): 3981. <https://doi.org/10.3390/molecules25173981>
- Kaya M, Lelešius E, Nagrockaitė R, Sargin I, Arslan G, Mol A, Baran T, Can E and Bitim B (2015), Differentiations of chitin content and surface morphologies of chitins extracted from male and female grasshopper species, *PLoS ONE* **10**: e0115531. <https://doi.org/10.1371/journal.pone.0115531>
- Machado SSN, da Silva JBA, Nascimento RQ, Lemos PVF, de Jesus Assis D, Marcelino HR, de Souza Ferreira E, Cardoso LG, Pereira JD, Santana JS, da Silva MLA and de Souza CO (2024), Insect residues as an alternative and promising source for the extraction of chitin and chitosan, *Int J Biol Macromol* **254**(3): 127773. <https://doi.org/10.1016/j.ijbiomac.2023.127773>
- Mei Z, Kuzhir P and Godeau G (2024), Update on chitin and chitosan from insects: Sources, production, characterization, and biomedical applications, *Biomimetics* **9**: 297. <https://doi.org/10.3390/biomimetics9050297>
- Milbreta U, Andze L, Zoldners J, Irbe I, Skute M and Filipova I (2025), Exploring the potential of locally sourced fungal chitosan for paper mechanical property enhancement, *J Renew Mater* **13**(3): 583-597. <https://doi.org/10.32604/jrm.2024.057663>
- Montgomery DC (2017), *Design and Analysis of Experiments*, 9th Ed. (Wiley, New Jersey), pp 752.
- Myers RH, Montgomery DC and Anderson-Cook CM (2016), *Response Surface Methodology: Process and Product Optimization Using Designed Experiments*, 4th Ed. (Wiley, New Jersey), pp 688.
- Ngomo O, Mafosso-Tanto A, Poughella S and Sieliechi J (2024), Optimization of deacetylation parameters during the extraction of chitosan from shrimp shells waste, *Open Access Libr J* **11**: 1-18. <https://doi.org/10.4236/oalib.1111706>
- Noura El-Far A, Yousseria MS, Ahmed MA, Rehab MA and Abdou DAM (2021), Statistical optimization of chitosan production using marine-derived *Penicillium chrysogenum* MZ723110 in Egypt, *Egypt J Aquat Biol Fish* **25**(5): 799-819.
- Olafadehan OA, Ajayi TO and Amoo KO (2020), Optimum conditions for extraction of chitin and chitosan from *Callinectes amnicola* shell waste, *Theor Found Chem Eng*. **54**: 1173-1194.
- Pakizeh M, Moradi A and Ghassemi T (2021), Chemical extraction and modification of chitin and chitosan from shrimp shells, *Eur Polym J* **159**: 110709. <https://doi.org/10.1016/j.eurpolymj.2021.110709>

- Rehman KU, Hollah C, Wiesotzki K, Heinz V, Aganovic K, Rehman RU, Petrusan JI, Zheng L, Zhang J and Sohail S (2023), Insect-derived chitin and chitosan: A still unexploited resource for the edible insect sector, *Sustainability* **15**: 4864. <https://doi.org/10.3390/su15064864>
- Reshad RAI, Jishan TA and Chowdhury NN (2021), Chitosan and its broad applications: A brief review, Available at SSRN 3842055. <https://doi.org/10.29333/jcei/11268>
- Struszczyk MH (2002), Chitin and chitosan. Part 1. Properties and production, *Polimery* **47**: 316-325.
- Teixeira-Costa BE and Andrade CT (2021), Chitosan as a valuable biomolecule from seafood industry waste in the design of green food packaging, *Biomolecules*. **11**: 1599. <https://doi.org/10.3390/biom11111599>
- Thakur R, Saberi B, Pristijono P, Stathopoulos CE, Golding JB, Scarlett CJ, Bowyer M and Vuong QV (2017), Application of chitosan films in food packaging: A review, *J Food Sci Technol*. **54**(8): 2270-2278. <https://doi.org/10.1007/s13197-017-2664-y>
- Tiama TM, Ismail AM, Elhaes H and Ibrahim MA (2023), Structural and spectroscopic studies for chitosan/Fe₃O₄ nanocomposites as glycine biosensors, *Biointerface Res Appl Chem*. **13**(6): 547-560. <https://doi.org/10.33263/BRIAC136.547>
- Triunfo M, Tafi E, Guarnieri A, Salvia R, Scieuzo C, Hahn T, Zibek S, Gagliardini A, Panariello L and Coltelli MB (2022), Characterization of chitin and chitosan derived from *Hermetia illucens*: A further step in a circular economy process, *Sci Rep*. **12**: 6613. <https://doi.org/10.1038/s41598-022-10423-5>
- Vaingankar PN and Juvekar AR (2014), Fermentative production of mycelial chitosan from zygomycetes: Media optimization and physico-chemical characterization, *Adv Biosci Biotechnol* **5**(12): 940-956. <https://doi.org/10.4236/abb.2014.512108>
- Verma C and Quraishi MA (2021), Chelation capability of chitosan and chitosan derivatives: Recent developments in sustainable corrosion inhibition and metal decontamination applications, *Curr Res Green Sustain Chem*, **4**: 100184. <https://doi.org/10.1016/j.crgsc.2021.100184>
- Wang J, Yuan Y, Liu Y, Li X and Wu S (2024), Application of chitosan in fruit preservation: A review, *Food Chem X*, **23**: 101589. <https://doi.org/10.1016/j.fochx.2024.101589>
- Zainol Abidin NA, Kormin F, Mohamed Anuar NAF and Abu Bakar MF (2020), The potential of insects as alternative sources of chitin: An overview on the chemical method of extraction from various sources, *Int J Mol Sci*. **21**(14): 4978. <https://doi.org/10.3390/ijms21144978>